DOI 10.1007/s11141-024-10314-x
Radiophysics and Quantum Electronics, Vol. 66, Nos. 7–8, December, 2023
(Russian Original Vol. 66, Nos. 7–8, July–August, 2023)

PULSED POWER AND SPECTRUM COMPOSITION OF THE TERAHERTZ RADIATION FLUX ESCAPING FROM A PLASMA COLUMN DUE TO PROPAGATION THROUGH IT OF A RELATIVISTIC ELECTRON BEAM WITH VARIOUS CURRENT DENSITIES (GOL–PET FACILITY EXPERIMENTS)

D. A. Samtsov,[1*] **A. V. Arzhannikov,**[1,2]
S. L. Sinitsky,[1,2] **P. V. Kalinin,**[1,2] **S. S. Popov,**[1]
E. S. Sandalov,[1,2] **M. G. Atlukhanov,**[1] **K. N. Kuklin,**[1]
M. A. Makarov,[1] **V. D. Stepanov,**[1,2] **and**
A. F. Rovenskikh [1]

UDC 533.922+537.531

One of the possible applications of high-current relativistic electron beams (REBs) is to generate electromagnetic waves at plasma frequencies due to the propagation of a beam through a magnetized plasma column. Research work in this direction, aimed at creating terahertz radiation sources at the BINP, is underway using the GOL–PET facility. We study the relaxation of a REB beam with a current density of (1–2) kA/cm^2 *in a magnetized plasma column with a density of* $5 \cdot 10^{14}$ cm^{-3}. *The purpose of these studies is to create a pulse radiation source with a power of tens of megawatts in the frequency range* 0.1–1 *THz. To date, a radiation flux with a power level of 10 MW and a maximum power spectral density in the frequency range* 150–200 *GHz has been achieved in the experiments. Further progress in these studies was related to the experimental establishment of the dependence of the power and spectral composition of the radiation flux on the parameters of the injected beam, in particular, its current density. The current density of the injected beam was varied due to the different compression of the beam cross section by the magnetic field. The results of measuring the characteristics of the radiation flux are presented in correlation with the results of measurements of the beam current density and plasma density.*

1. INTRODUCTION

One of the key branches of the physics of relativistic electron beams (REBs) is related to the study of features of their propagation in free space and in a plasma in regard to the possibility of generating electromagnetic radiation for the purpose of subsequent creation of high-power sources for various frequency ranges [1–3]. In the case of using REBs to generate radiation in vacuum electrodynamic systems, a usable beam current is limited by the potential sag over the beam cross section. Therefore, the power level of the radiation generated in a device with axially symmetric geometry turns out to be very limited [1], especially when moving into the millimeter wavelength range. One way of overcoming this obstacle is the transition to the planar geometry of an electrodynamic system, using a sheet beam [4, 5], which has already made it possible to generate radiation with a megawatt power level in the millimeter wavelength range [6]. A fundamentally new solution of the problem on the sag of the potential in the beam cross section was the

* d.a.samtsov@inp.nsk.su

[1] G. I. Budker Institute of Nuclear Physics of the Siberian Branch of the Russian Academy of Sciences; [2] Novosibirsk State University, Novosibirsk, Russia. Translated from Izvestiya Vysshikh Uchebnykh Zavedenii, Radiofizika, Vol. 66, Nos. 7–8, pp. 595–605, July–August 2023. Russian DOI: 10.52452/00213462_2023_66_07_595 Original article submitted May 15, 2023; accepted August 1, 2023.

transition to generation of millimeter- and submillimeter-wave radiation of a high-current REB under conditions of its propagation in the plasma. The presence of the plasma medium ensures the beam neutralization not only with respect to the local electrostatic field created by the beam electrons, but also with respect to the local current density, which almost completely removes limitation on the total beam current used for the generation of radiation [3]. Frequency spectrum of the radiation flux generated in the beam–plasma system is determined by the plasma density and the induced magnetic field guiding the beam. A spectral range of 0.1 to 0.5 THz has been mastered in the experiments performed to date [7]. Increased plasma density during the study of the beam–plasma interaction will shift the generation of radiation to the range of even higher frequencies, and such studies, which are of fundamental nature, of course, should receive further development. The creation of beam–plasma oscillators using modern engineering and technical solutions for pulsed high-current accelerators and systems for producing a dense plasma brings these devices into the field of practical applications even today. Radiation fluxes with a wide spectral composition in the discussed frequency range make it possible to (i) analyze and modify the structure of composite materials, complex metal–dielectric objects, and supramolecular structures, (ii) search for and visualize hidden objects under clothing or weakly conductive shelters, (iii) detect and visualize small objects at kilometer distances, and (iv) perform submillimeter spectroscopy of fast processes. Studies aimed at pumping of energy levels in the basin of phonon oscillations of complex supramolecular structures are of particular interest.

The general principle of operation of such beam–plasma systems is as follows. When the beam propagates in a plasma with the beam electron velocity coinciding with the phase velocity of the electron plasma oscillations, a Čerenkov resonance arises between them under certain conditions, which ensures the emergence and development of the beam (or, in other words, two-stream) instability [8–10]. As a result, when the beam passes through the plasma, a significant fraction of the electron energy is spent on excitation and subsequent pumping of Langmuir, or upper-hybrid plasma oscillations [11]. Then, depending on a particular configuration of the beam–plasma system and its parameters, the mechanisms of transformation of these plasma waves into electromagnetic ones are realized. A detailed consideration of these mechanisms in regard to using kiloampere REBs to obtain high-power radiation fluxes at the upper-hybrid frequency and its double value was carried out in [7, 12, 13]. Note that in the studies of electromagnetic wave generation using the beam–plasma system there is another direction in which the spectral properties of a thin plasma slab are employed to control of frequency-selective characteristics of an axially symmetric electrodynamic system in a wavelength range of about 10 cm [14].

This paper gives the results of a series of experimental studies of radiation generation in the range 0.1–0.4 THz, which were performed using the GOL–PET facility at the G. I. Budker Institute of Nuclear Physics (BINP) of the Siberian Branch of the Russian Academy of Sciences. These studies used a plasma column with a density of $(2\text{–}6)\cdot 10^{14}\,\mathrm{cm}^{-3}$, which is confined in a multi-mirror magnetic trap with an average field of about 4 T. A relativistic electron beam with the following parameters was used for pumping of plasma oscillations: current 40 kA, particle energy 0.4–0.5 MeV, and duration 5 μs. The main objective of this research is to determine plasma parameters and REB injection conditions under which a high-power directed flux of electromagnetic radiation is generated [15, 16]. To date, conditions have already been created under which the generation of submillimeter-wave radiation of microsecond duration with a record-breaking (10 MW) power level in the flux released into the atmosphere was achieved [17]. In these experiments, performed in the presence of a strong magnetic field, the beam is used to pump upper-hybrid plasma waves, which, transforming at local plasma-density gradients, exit from the plasma column in the form of a flux of electromagnetic radiation at the frequency of the initial plasma wave [3]. In addition, the process of merging of two oscillations into one electromagnetic wave with doubled upper-hybrid frequency [13] is possible at a high pumping level of these upper-hybrid oscillations. Moreover, a possibility for direct pumping of the electromagnetic branch of plasma oscillations by the beam opens up in the case of a quasiperiodic disturbance of the plasma density over the radius of the plasma column and along its axis [7]. It should be noted that to achieve a high efficiency of radiation generation in the experiments, a high level of plasma oscillations is required, which can lead to their irregular behavior in time, being accompanied by fluctuations in the power

and spectral composition of the generated flux. For this reason, special attention was paid in the experiments to seeking conditions for time-stable generation of the radiation flux.

The record-breaking power parameters achieved to date in the radiation flux and the understanding of the plasma wave transformation processes make it possible to formulate new research problems. One of such problems was to master the frequency range 0.5–0.9 THz, the solution of which requires an increase in plasma density and in the current density of the electron beam. For example, generation of radiation at a plasma frequency of about 0.6 GHz becomes possible with a plasma density of $1.6 \cdot 10^{15}\,\mathrm{cm}^{-3}$ and a beam current density of $4\,\mathrm{kA/cm}^2$. One way to increase the current density of the beam is to reduce its cross section by compression in a magnetic field. To obtain an electron beam with the required current density, we consider the possibility of using the injector of the linear induction accelerator developed at the BINP [18, 19]. This accelerator ensures the generation of an electron beam with a particle energy of 2 MeV and a current of 2 kA with a pulse duration of 120 ns. The advantage of this accelerator over the direct accelerator U-2, which is currently used, is the high brightness of the beam generated in the diode, which makes it possible to achieve a high density of the current by compressing its cross section during injection into the plasma. It is exactly a low emittance of the generated beam that provides the possibility of compressing the beam cross section down to a diameter of several millimeters [19]. Due to this, the problem has arisen to determine how the degree of compression of the beam cross section, which increases the beam current density during injection into the plasma, affects the parameters of the terahertz radiation flux generated in the plasma column.

Earlier, during a study of radiation generation in the beam–plasma system, the influence of a uniform decrease in the guiding field on the power and spectral composition of the generated radiation was considered as a function of the configuration of the guiding magnetic field [20]. This paper focuses on studying the influence of the degree of compression of the REB before its injection into the plasma column on the radiation generation processes. The spectral composition of the radiation was measured with different magnetic-field ratios in the diode and in the solenoid.

2. DESCRIPTION OF THE GOL–PET FACILITY AND OPERATION SEQUENCE OF ITS SYSTEMS

Experimental studies are performed using the GOL–PET facility, which consists of a U-2 accelerator, which generates a high-current REB, and a plasma section, the schematic diagram of which is shown in Fig. 1. Preliminary (target) plasma is formed as follows. First of all, neutral gas is injected into the vacuum volume using a system of quick pulsed valves *1* and *2*. Two types of gas, hydrogen and krypton, are used. The required distribution of these gases along the length of the vacuum chamber is achieved by specifying the type of gas and its pressure in each valve before experiments and by setting the opening and closing times of each valve during the pulses. The characteristic time that is necessary to fill the chamber and achieve the required gas concentration profiles is about 15 ms. These profiles are presented in Fig. 1 in the bottom diagram of the gas concentration distribution along the length of the vacuum chamber (along the z axis). Krypton is injected into the compression system of the beam cross section (purple line in the diagram) in order to provide the necessary neutralization of the own charge of an electron beam during its compression, as well as to block the propagation of hydrogen along the axis in the direction of the accelerator diode from the plasma column confined in the solenoid. Hydrogen is injected at the entrance of the vacuum chamber (blue line) and in its central part at the distance $z = 84$ cm from its entrance (red line).

A plasma discharge is formed by controlled initiation of breakdown in a neutral hydrogen released through the valves. To achieve a high-voltage hydrogen breakdown, a pair of ring electrodes *3* is mounted inside the chamber. A voltage of 25 kV is applied to them from a capacitor bank with a total capacity of 3.2 μF as a result of controlled operation of the ignitron. To confine the plasma in the chamber, a solenoid creating a multimirror magnetic-field configuration is used. Corrugation period in the described experiments was 22 cm, with a maximum-to-minimum field ratio of 1.4. Injection of the REB into the column of preliminarily prepared plasma was performed 20 μs after the occurrence of a discharge current, which corresponded to one period of the current oscillations. The energy of injected electrons is determined by the voltage applied

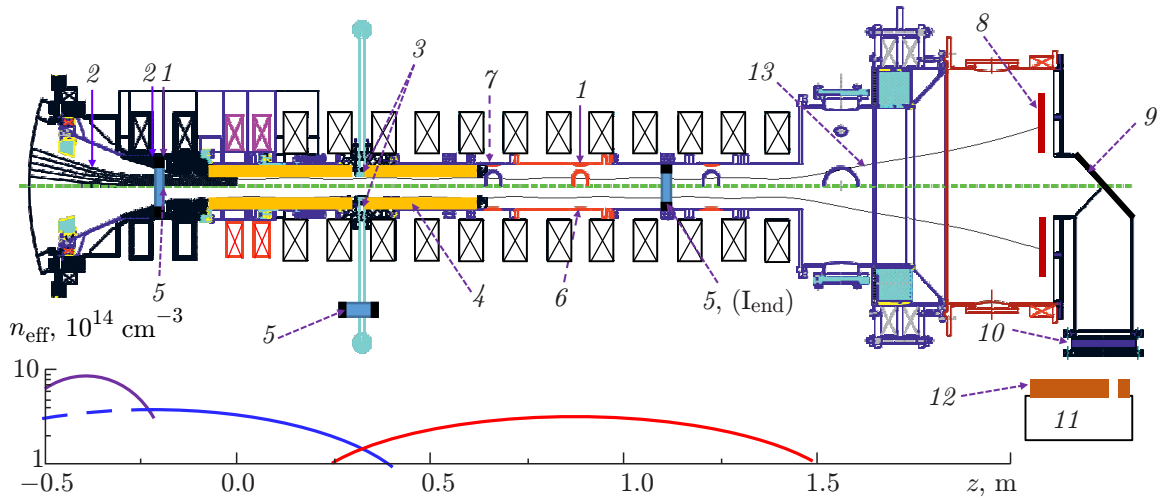

Fig. 1. Scheme of the plasma section of the GOL–PET facility: valves for the injection of hydrogen and krypton (*1* and *2*, respectively), high-voltage electrodes (*3*), quartz pipe (*4*), Rogowski belts (*5*), interferometer (*6*), Thomson scattering node (*7*), graphite collector (*8*), rotating mirror (*9*), output window (*10*), polychromator (*11*), neon light panel (*12*), and magnetic field lines (*13*). The distributions of the gas density over the length of the vacuum chamber are shown on the bottom.

to the accelerator diode and can be varied in the range 0.4–0.8 MeV. It should be noted that the magnetic system that provides guidance of the beam from the accelerator diode to the plasma column is composed of individual coils, each being driven by the current from a separate capacitor unit. The first block ensures a magnetic field in a magnetically insulated accelerator diode, the second, a magnetic field in the system for transformation and compression of the beam cross section before the beam is injected into the plasma, and the third ensures a magnetic field in the solenoid and expander, where the beam is absorbed at the graphite collector. The degree of compression of the REB was changed by varying the charging voltage of individual capacitor-bank units and, accordingly, current in the coils. In this series of experiments, the charging voltage of the first and second capacitor-bank units was jointly adjusted, and the third unit, independently of the first two. Thus, the guiding magnetic field configuration determining the degree of REB compression was varied in the experiments. A sharp decrease in plasma density and a strong decrease in the magnetic field were achieved in the expander area. On the one hand, this provides unhindered output of the generated flow of electromagnetic radiation along the axis of the facility, and on the other hand, a decrease in the density of the REB current at the receiving collector due to the expansion of the beam cross section in the decaying field. Thus, the main fraction of the beam electrons is absorbed on the graphite collector *8*, and the longitudinal terahertz radiation flux is passes through a hole with a diameter of 16 cm and then propagates to the rotating mirror *9*, which is mounted at an angle of 45° to the axis of the facility. Then this radiation flux is reflected from mirror *9* and is released into the atmosphere through output window *10*.

To measure the main parameters of the plasma column and the beam of relativistic electrons, as well as for recording characteristics of the radiation flux, the following set of diagnostic methods is used. To measure the plasma density, optical diagnostic tools, such as a Michelson interferometer *6* at a wavelength of 10.5 μm and a Thomson scattering system *7* at a wavelength of 1.053 μm, are employed. High-voltage discharge current and the beam current are measured using a set of Rogowski coils *5*. To estimate the electron temperature of the beam-heated plasma, diamagnetic loops are used. The cross section of the radiation flux released into the atmosphere is recorded by the glow of a panel of neon light bulbs *12*, and the spectral composition of the radiation is determined using an 8-channel polychromator *11*. This device is based on radiation detectors in the frequency range 0.1–0.6 THz, which are Schottky-barrier semiconductor diodes with the frequency-selective bandpass filters mounted in front of them [21].

TABLE 1. Variants of the guiding magnetic field distribution in different parts of the facility.

No.	Average field in the accelerating diode, T	Average field in the plasma column, T	Ratio of the fields
1	0.40	4	10
2	0.25	2.5	10
3	0.25	3.4	14
4	0.25	4	16

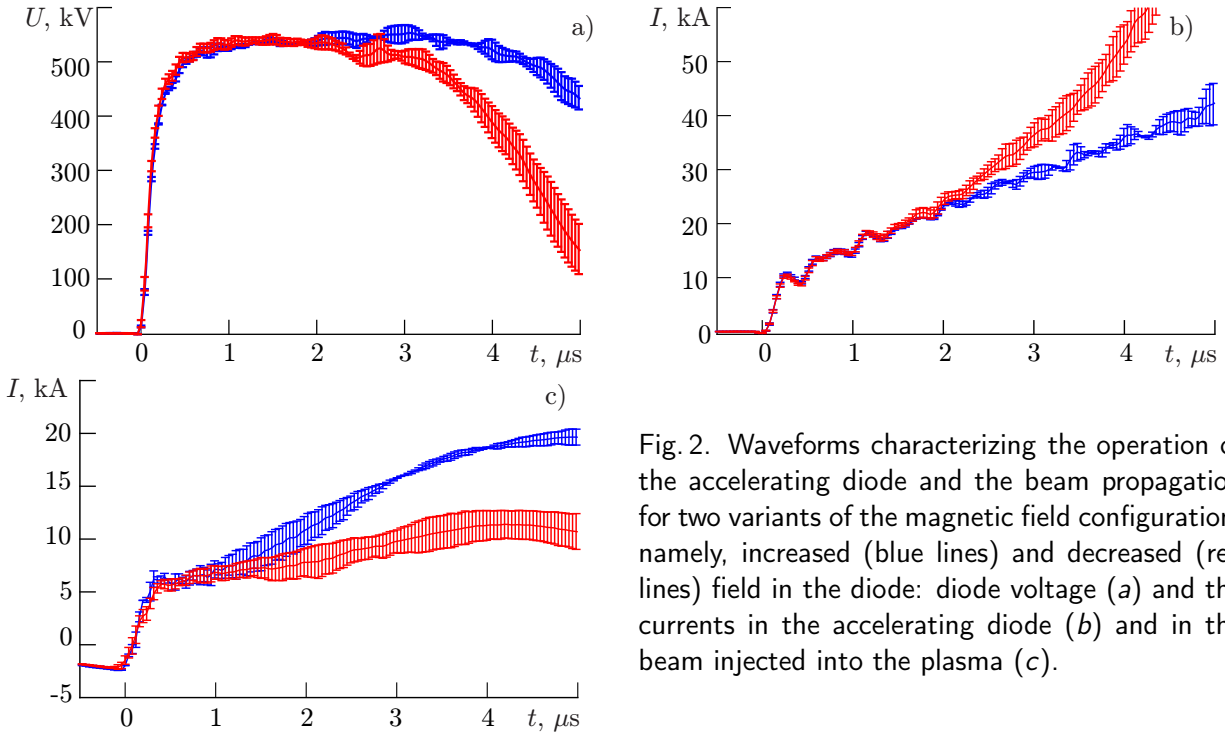

Fig. 2. Waveforms characterizing the operation of the accelerating diode and the beam propagation for two variants of the magnetic field configuration, namely, increased (blue lines) and decreased (red lines) field in the diode: diode voltage (*a*) and the currents in the accelerating diode (*b*) and in the beam injected into the plasma (*c*).

3. EXPERIMENTS WITH VARYING THE LONGITUDINAL PROFILE OF THE MAGNETIC FIELD

This paper focuses on studying the influence of the degree of the REB compression before the beam is injected into the plasma column on the radiation generation process. It was noted in the previous section that the longitudinal profile of the guiding magnetic field was varied by changing the charging voltage of the capacitor-bank units that supply the coils. Space-averaged values of the magnetic field in the accelerating diode and in the vacuum chamber with a plasma column for different variants of the magnetic field distribution over the length of the facility are given in Table 1.

Earlier, in the course of studying the influence of the strength of the guiding magnetic field on the generation (power and spectral composition) of radiation in the beam–plasma system, we gradually moved from variant 1 to variant 2 by uniformly reducing the field along the entire length of the facility [20]. Then, to implement variants 2–4, the guiding field was gradually increased only in the solenoid of the plasma section of the facility, which corresponded to an increase in the REP compression factor. However, we note the following characteristic difference in configurations with reduced (variant 2) and non-reduced (variant 1) fields in the diode. Figure 2 shows waveforms of the accelerating-diode voltage and the beam current measured by Rogowski coils in different sections of the vacuum chamber for two variants of the diode field.

It is seen from the waveforms in Figs. 2*a* and 2*b* that the reduction of the guiding field in the diode leads to an increase in the rate of growth of the diode current, which is accompanied by a decrease in the duration of REB generation. Herein, there is a decrease in the current of the beam injected into the plasma column (see Fig. 2*c*). We relate this behavior of the current to the following reasons. Before injection into

the plasma column, an electron beam undergoes cross-sectional compression in an increasing magnetic field, in which it needs to pass through a magnetic mirror. The condition of passing imposes a constraint on the maximum pitch angle of the electron, which is given by the formula $\theta_m = \sin^{-1}(\sqrt{B_1/B_2})$, where B_1 and B_2 are the fields in the diode and the solenoid mirror, respectively. Reducing the guiding field in the diode leads to an increase in the angular spread of electron velocities in the beam [22] and, as a consequence, increases the fraction of electrons reflected from the magnetic mirrors of the solenoid back into the accelerating diode. Thus, the reduction of the diode field in order to provide additional beam compression does not lead to an increase in the beam current passing into the plasma column due to the deterioration of angular characteristics of the beam electrons and an increase in the fraction of electrons reflected from the magnetic mirror of the solenoid back into the diode. Moreover, an increase in diode current causes a sharp decrease in dynamic resistance of the diode gap and, as a consequence, decreases the duration of the pulse of the REB generated in the diode.

It should also be noted that the dependence of the plasma density on time changes during the beam injection for all field configurations with increased ratio of the field in the plasma to the field in the diode. The dependence of the average plasma density across the column diameter on time for regimes with standard and increased compression of the beam cross section is given in Fig. 3. It can be seen in this figure that in the case of increased magnetic field in the diode (the beam cross-sectional compression factor $k = 10$ and the diameter of the compressed beam in the plasma is 6 cm), the plasma density in the plasma column starts to increase 0.5 μm after the start of the REB injection, and the diameter-average plasma density reaches $(7–8) \cdot 10^{14}$ cm^{-3} on a time scale of 4 μs. In the case of a low field in the diode (the factor $k = 16$), when the diameter of the compressed beam in the plasma is 4.8 cm, the plasma density starts to increase later, only 1 μs after the start of REB injection, and the average plasma density reaches $(3–4) \cdot 10^{14}$ cm^{-3} within 4 μs.

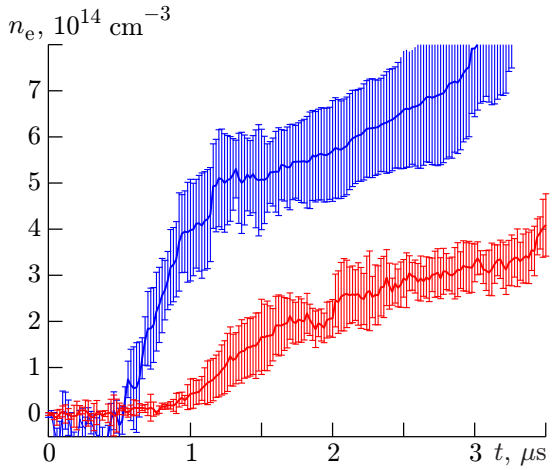

Fig. 3. Diameter-average plasma density in the cross section $z = 84$ cm, determined from the results of recording by a Michelson interferometer, for two variants, namely, increased (blue line) and decreased (red line) fields in the diode.

Implemented variants for changing the configuration of the guiding magnetic field with increased compression of the beam cross section leads, on the one hand, to some decrease in the beam current passing into the plasma column through the magnetic mirror (due to the reflection from it of electrons with high pitch angles). On the other hand, the injected beam that has passed into the plasma column has a smaller angular spread of particle velocities and increased current density due to the decrease in its cross section.

The reduction in the beam cross section was sufficient, so that the beam did not touch the limiting irises when it propagated along the plasma column. Under these conditions, there was no entry of evaporated iris substance into the plasma, which increased the interferometer signal characterizing the plasma density integrated over the diameter (blue line of the behavior of the diameter-average integral plasma density in Fig. 3). As a result, at a high ($k = 16$) degree of compression of the beam cross section, the integral cross-sectional plasma density does not increase as significantly, and its maximum value gives an average plasma density not exceeding $3 \cdot 10^{14}$ cm^{-3} during the generation of radiation, which corresponds to the density of molecular hydrogen injected into the chamber.

Next, we proceed to analyzing the spectrum of radiation generated in a series of experiments with varying the degree of REB compression. Using an 8-channel polychromator at a fixed beam compression factor, we measured the spectral density of the radiation flux released into the atmosphere. In accumulated results of recording, exactly those of them that were obtained under identical conditions with respect to plasma parameters were selected and averaged. Figure 4 shows the results of averaging signals over a series

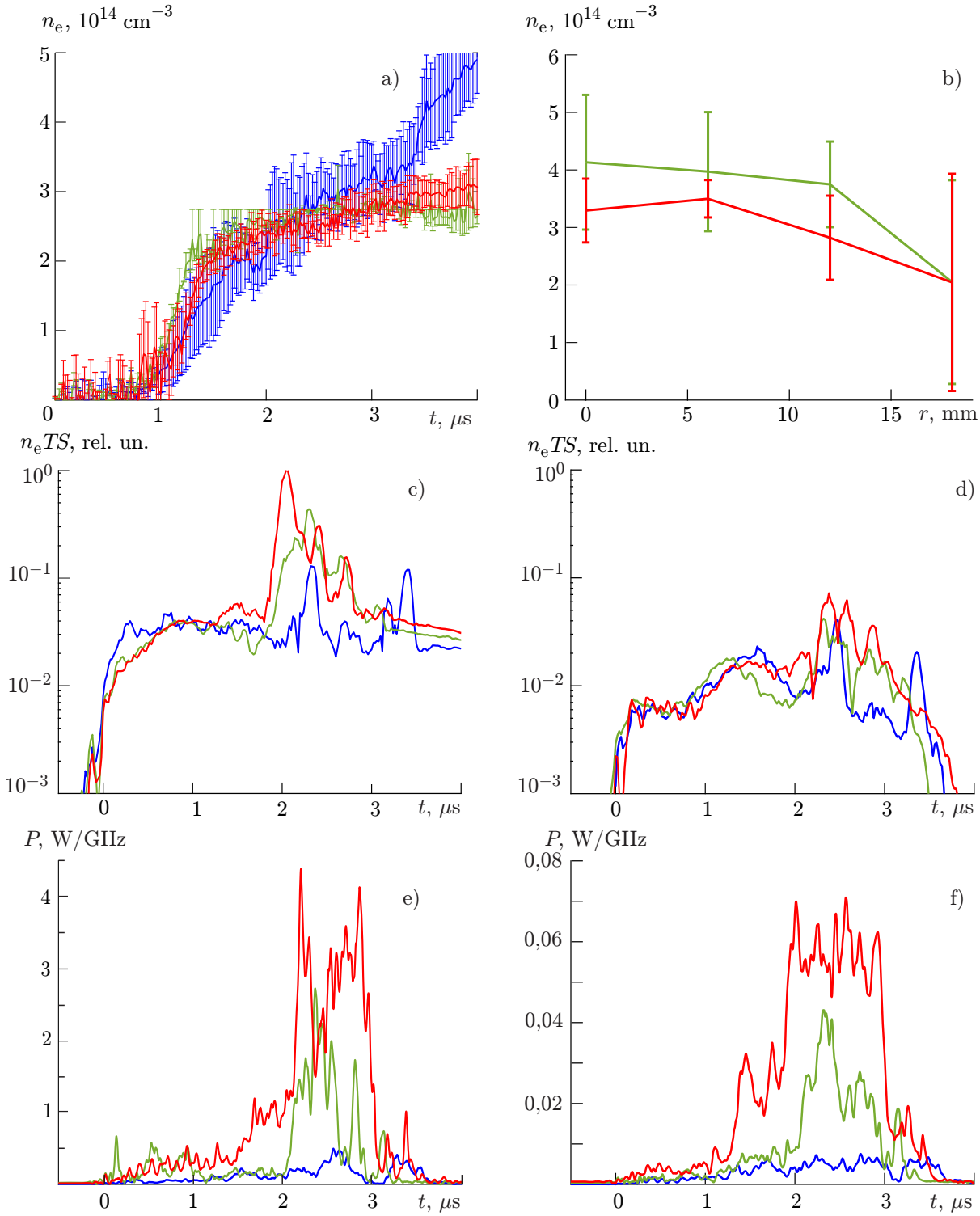

Fig. 4. The sensor signals averaged over a series of identical shots with REB injection, which characterize the time behavior of the state of the plasma column and the generated radiation flux: average plasma density across the column diameter (*a*), local plasma-density profile across the column radius, measured at a time of 3 μs (*b*), diamagnetic signal of the plasma in the cross sections $z = 45$ cm (*c*) and 120 cm (*d*), and the radiation signals from the polychromator channels, which correspond to the frequencies 150 GHz (*e*) and 440 GHz (*f*). The blue, green, and red curves correspond to the REB cross-sectional compression factors $k = 10$, 14, and 16.

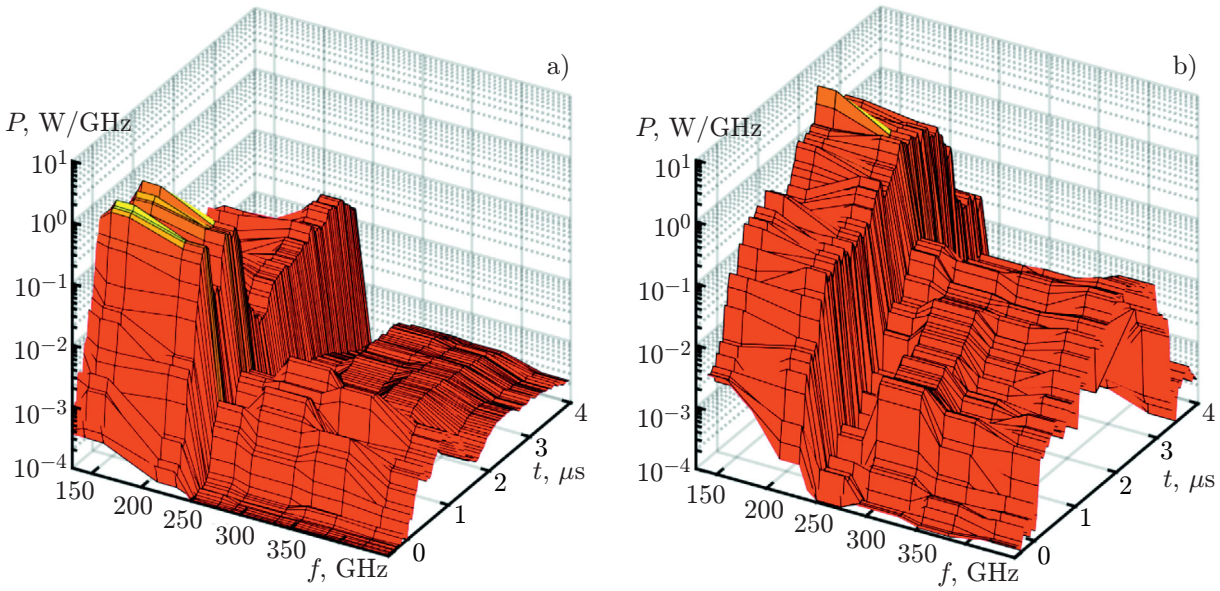

Fig. 5. Comparison of the spectra for two configurations of magnetic fields with weak (*a*) and strong (*b*) compression of the REB cross section, which are given in Table 1 (variants 1 and 4, respectively).

of beam shots with similar parameters. Here are the results of measurements of the plasma density n_e, the diamagnetic plasma signal n_eTS, where T is the electron temperature and S is the plasma cross-sectional area, and the spectral radiation power P at frequencies of 150 and 440 GHz.

The presented results on radiation generation clearly show the existence of two spectral regions, a low-frequency one (100–250 GHz) and a high-frequency one (300–450 GHz). It can be seen in Fig. 4*a* that by the time 1.5 μs from the start of the beam injection, the process of additional rise in plasma density is over and then its distribution over the column radius becomes uniform. Note that the plasma density depends only weakly on the degree of REB compression, as shown in Figs. 4*a* and 4*b*. We assume that the cessation of the plasma density increase is due to the achievement of complete ionization of hydrogen in a given cross section of the plasma column. The electron temperature starts to increase abruptly in 2 μs, as demonstrated by the results of measuring the pressure in the plasma, which is characterized by signals from diamagnetic loops in the cross sections $z = 45$ cm (Fig. 4*c*) and $z = 120$ cm (Fig. 4*d*). Note that the increase in diamagnetism is more pronounced in the initial region of the plasma column. Moreover, it follows from diamagnetic signals that a significant increase in plasma pressure is observed in a time interval in which the power in the radiation flux rises abruptly in both frequency ranges (see the signals in Figs. 4*e* and 4*f*).

It is seen in Figs. 4*e* and 4*f* that under conditions of increased compression of the REB cross section, the power in the radiation flux rises in 2 μs and reaches the maximum values closer to the end of the pulse (2.5 μs). Moreover, with the increase in the compression factor of the REB cross section at a constantly low field in the diode, there is a proportional increase in peak radiation power. In this regard, in cases with REB compression factors $k = 14$ and 16, a two-layer diaphragm with a hole of 60 mm in diameter was placed behind the output window of the facility with a diameter of 140 mm to reduce the power level in the polychromator channel to acceptable values. The top layer was made of foam rubber saturated with graphite, which absorbs terahertz radiation, and the bottom one was made of conductive foil reflecting that radiation. Note that the input window of the polychromator, which was located at a distance of 1 m from the output window of the vacuum chamber was 85 mm in diameter.

Averaged signals from the polychromator channels were used to retrieve the power spectral density distribution in the radiation flux released into the atmosphere. Figure 5 shows the radiation spectra corresponding to two variants of magnetic fields (see variants 1 and 4 in Table 1).

It is seen from the spectra presented that an increase in the current density in a beam by additional compression of its cross section by a magnetic field leads to changing the dynamics of the radiation flux

formation. In regimes with additional compression of the REB, the maximum power in the radiation flux shifts at a time of about 2.5–3.0 μs, i. e., moves to the end of the electron-beam injection pulse. An increase in the compression factor from 10 to 16 leads to a significant (fivefold) increase in the power of generated radiation flux. Although the maximum power is still localized in the plasma frequency range (150–200 GHz), the relative fraction of radiation power localized in the range of high (300–400 GHz) frequencies, which corresponds to the doubled fundamental plasma frequency, also increases.

4. CONCLUSIONS

We have studied the spectrum of terahertz radiation at the output of the plasma column for different current densities of the injected REB. The current density was varied by changing the longitudinal profile of the guiding magnetic field. The change in the current density was accompanied by changes in the beam cross section and in the angular divergence of the beam electron velocities. A change in the radiation generation was detected in the experiments when the REB compression factor was increased from 10 to 16. The field reduction in the accelerator diode, achieved in the experiments, leads to a decrease in the duration of beam generation, but favors that the beam passes through the plasma with a reduced cross-sectional diameter and does not touch the irises limiting the plasma column. In these conditions, the plasma column has a given density during the main time interval for which the beam passes through the column. With increased compression of the REB cross section ($k = 16$), the maximum power in the radiation flux is reached at the moment of time about 2.5–3.0 μs, which corresponds to the time shift of the maximum to the end of the beam injection pulse compared to the case $k = 10$. An increase in the degree of compression of the beam cross section due to an increase in the ratio between the magnetic field in the plasma column and the field in the accelerator diode up to $k = 16$ leads to a significant (fivefold) increase in the flux power of the generated radiation. The maximum spectral density of the radiation flux power is still localized in the plasma frequency range (150–200 GHz). In this case, the relative fraction of power, localized in the range of the doubled plasma frequency (300–400 GHz), also increases.

This work was supported by the Russian Science Foundation (project No. 19–12–00250–P).

REFERENCES

1. M. Yu. Glyavin, G. G. Denisov, V. E. Zapevalov, et al., *J. Commun. Technol. Electron.*, **59**, No. 8, 792–797 (2014). https://doi.org/10.1134/S1064226914080075
2. A. I. Klimov, S. D. Korovin, V. V. Rostov, and E. M. Tot'meninov, *Tech. Phys. Lett.*, **32**, No. 2, 120–122 (2006). https://doi.org/10.1134/S106378500602009X
3. A. V. Arzhannikov, A. V. Burdakov, P. V. Kalinin, et al., *Vestnik Novosibirsk Univ., Ser. Fiz.*, **5**, No. 4, 44–49 (2010).
4. N. S. Ginzburg, N. Y. Peskov, A. S. Sergeev, et al., *Phys. Rev. E*, **60**, No. 1, 935–945 (1999). https://doi.org/10.1103/PhysRevE.60.935
5. A. V. Arzhannikov, N. S. Ginzburg, V. Yu. Zaslavsky, et al., *JETP Lett.*, **87**, No. 11, 618–622 (2008). https://doi.org/10.1134/S0021364008110052
6. A. V. Arzhannikov, N. S. Ginzburg, P. V. Kalinin, et al., *Phys. Rev. Lett.*, **117**, No. 11, 114801 (2016). https://doi.org/10.1103/PhysRevLett.117.114801
7. A. V. Arzhannikov, I. A. Ivanov, A. A. Kasatov, et al., *Plasma Phys. Control. Fusion*, **62**, No. 4, 045002 (2020). https://doi.org/10.1088/1361-6587/ab72e3
8. A. I. Akhiezer and Ya. B. Fainberg, *Dokl. Akad. Nauk SSSR*, **69**, No. 3, 555–561 (1949).
9. A. V. Arzhannikov, A. V. Burdakov, V. S. Koidan, et al., *Phys. Scr.*, **T2/2**, 303–310 (1982).
10. A. A. Vedenov and L. I. Rudakov, *Sov. Phys. Dokl.*, **9**, 1073–1076 (1964).

11. B. N. Breizman, D. D. Ryutov, and P. Z. Chebotaev, *Sov. Phys. JETP*, **35**, No. 4, 741–747 (1972).

12. A. V. Arzhannikov and I. V. Timofeev, *Vestnik Novosibirsk Univ., Ser. Fiz.*, **11**, No. 4, 78–104 (2016).

13. A. V. Arzhannikov and I. V. Timofeev, *Plasma Phys. Control. Fusion*, **54**, No. 10, 105004 (2012). https://doi.org/ 10.88/1741-3335/54/10/105004

14. P. S. Strelkov, *Phys. Usp.*, **62**, No. 5, 465–486 (2019). https://doi.org/10.3367/UFNe.2018.09.038443

15. V. V. Glinsky, I. V. Timofeev, V. V. Annenkov, and A. V. Arzhannikov, *Sib. Fiz. Zh.*, **14**, No. 4, 5–16 (2019). https://doi.org/10.25205/2541-9447-2019-14-4-5-16

16. D. A. Samtsov, A. V. Arzhannikov, S. L. Sinitsky, et al., *IEEE Trans. Plasma Sci.*, **49**, No. 11, 3371–3376 (2021). https://doi.org/10.1109/TPS.2021.3108880

17. A. V. Arzhannikov, S. L. Sinitsky, S. S. Popov, et al., *IEEE Trans. Plasma Sci.*, **50**, No. 8, 2348–2363 (2022). https://doi.org/10.1109/TPS.2022.3183629

18. A. V. Arzhannikov, S. L. Sinitsky, D. A. Starostenko, et al., in: *Proc. 5th Int. Conf. "Terahertz and Microwave Radiation: Generation, Detection and Application" (TERA-2023), February 27–March 2, 2023, Moscow, Russia*, pp. 46–47. https://doi.org/10.59043/9785604953914_46_2

19. D. A. Nikiforov, A. V. Petrenko, S. L. Sinitsky, et al., *J. Instrum.*, **16**, No. 11, P11024 (2021). https://doi.org/10.1088/1748-0221/16/11/P11024

20. D. A. Samtsov, A. V. Arzhannikov, S. L. Sinitsky, et al., *Radiophys. Quantum Electron.*, **65**, Nos. 5–6, 313–322 (2022). https://doi.org/10.1007/s11141-023-10214-6

21. S. A. Kuznetsov and A. V. Gelfand, *Russ. Phys. J.*, **58**, 1605–1612 (2016). https://doi.org/10.1007/s11182-016-0690-2

22. A. V. Arzhannikov, M. A. Makarov, D. A. Samtsov, et al., *Nucl. Instrum. Meth. Phys. Res. A*, **942**, 162349 (2019). https://doi.org/10.1016/j.nima.2019.162349